

Journal of Materials Chemistry B

Accepted Manuscript



This is an *Accepted Manuscript*, which has been through the Royal Society of Chemistry peer review process and has been accepted for publication.

Accepted Manuscripts are published online shortly after acceptance, before technical editing, formatting and proof reading. Using this free service, authors can make their results available to the community, in citable form, before we publish the edited article. We will replace this *Accepted Manuscript* with the edited and formatted *Advance Article* as soon as it is available.

You can find more information about *Accepted Manuscripts* in the [Information for Authors](#).

Please note that technical editing may introduce minor changes to the text and/or graphics, which may alter content. The journal's standard [Terms & Conditions](#) and the [Ethical guidelines](#) still apply. In no event shall the Royal Society of Chemistry be held responsible for any errors or omissions in this *Accepted Manuscript* or any consequences arising from the use of any information it contains.

ARTICLE

Hierarchical bioglass scaffolds: introducing the “milky way” for templated bioceramics.

Cite this: DOI: 10.1039/x0xx00000x

Diego Onna^a, Yanina Minaberry^a and Matías Jobbágy^{*a}.Received 00th January 2012,
Accepted 00th January 2012

DOI: 10.1039/x0xx00000x

www.rsc.org/

Free standing hierarchical bioglass scaffolds were prepared by ISISA (ice-segregation-induced self-assembly) method. Commercial low-cost precursors as Ludox[®] HS-40 and cow milk were employed as the source of SiO₂ and biominerals (Ca(II), P(V), Na(I) and K(I)), respectively. Then, in a single macroscopic piece, three levels of porosity coexist due to the simultaneous templating effect of ice (macropores), milk (50-200 nm mesopores) and the voids left between preformed Ludox[®] nano building blocks (2-5 nm mesopores). These low cost and green biological nanotemplates, coupled with ISISA texturing method allows the preparation of free standing bioglass monoliths, with hierarchical porosity. The effect of the main preparative variables on the final texture is explored; *in vitro* biomineralization ability revealed a well-distributed hydroxyapatite-like nanoparticulated layer within 24h-long exposure to simulated body fluid.

Introduction

The synthesis of biomaterials for bone-repair engineering triggered challenges for materials science community over the last decade. In the beginnings, bones were replaced by synthetic calcium phosphate phases. Later on, a vast family of non-natural occurring synthetic phases based on silica, known as bioactive glasses or bioglasses, offered outstanding regenerating abilities.¹⁻³ Typically, these formulations are based on Si(IV), P(V), Ca(II) and alkaline oxides, in order to optimize bioactivity, that is defined as the ability of the material to develop a bone-like hydroxyapatite (HA) layer on its surface.¹ These phases offered enhanced angiogenesis ability^{4, 5} as well as up-regulation of specific genes that control the osteoblast cell cycle,^{6, 7} among other relevant characteristics.⁸ Concerning their synthesis, sol gel based procedures allows the preparation of outstanding bioglasses, since silica polymerizes in intimate mixture with phosphate and calcium ions, preventing the massive undesired segregation of calcium phosphate.⁹⁻¹² Their composition was thoroughly explored and optimized in the past; during the last decade most efforts were focused on their consolidation in the form of sophisticated architectures,¹³ in order to enhance their regeneration ability with the aid of 3D biodegradable and biocompatible scaffolds. In this sense, a robust and well interconnected macroporous 3D network is mandatory, since it allows cellular proliferation while ensures effective mass transport between the inner growing tissue and the surrounding physiological media.¹⁴⁻¹⁷ In addition to macroporosity, the presence of tuned mesoporosity is highly desired, since it expands the functionality of the final bioglasses allowing advanced drug carrier/release or enhanced blood coagulation properties.¹⁸⁻²¹ Many approaches were proposed to texture bioglasses in the macropore scale, including *in situ* foam generation,^{22, 23} sacrifice natural²⁴ or synthetic²⁵⁻²⁷

template filling, electrospinning,²⁸ or robotic deposition (3D print).^{29, 30} More recently, the ISISA (ice-segregation-induced self-assembly) method was implemented for the preparation of bioglass monoliths with highly oriented macroporous texture.³¹ The process involves the controlled ice formation within an aqueous gel, solution or suspension, driving the segregation of all solutes and colloids present towards the zones in which the ice is absent. Macroporosity is achieved after ice sublimation, when a hierarchical assembly either defined by walls, fibers or bicontinuous arrays of matter surrounding empty areas where the ice formerly resided. Concerning bioglass preparation, most of the aforementioned methods are based on the utilization of expensive sol-gel precursors for silica or even phosphate, in combination with molecular templates. However, the inherent versatility of ISISA allows the incorporation of already consolidated precursors, in the form of nanoentities (particles, liposomes, polymers, etc.)³² resulting in diverse macroporous monolithic structures, ranging from strictly ceramic phases, to living-cell loaded polymeric composites.³³⁻³⁷ Keeping in mind this lack of chemical constrains, we envisaged an alternative low cost bioglass scaffold preparation, based on the structuration of preformed silica nanoparticles (Ludox[®] HS40) and commercial cow milk. While the former acts as dispersible source of SiO₂, the role of the latter is two-fold. First, it brings to the formulation a natural source of Ca(II) and P(V) among other biominerals as K(I) and Na(I). Second, the constituent liposomes and proteins act as sacrifice templating agents in the submicrometric scale, once the scaffolds are annealed and consolidated under air atmosphere.

The aim of the present work is to demonstrate that commercial low-cost precursors combined with green biological nanotemplates allow the preparation of hierarchical bioglasses with tunable porosity. The effect of ISISA main preparative variables on the bioglass texture as well as the subsequent

thermal treatment are explored. The influence on the *in vitro* biomineralization ability of the precursor's composition is also discussed.^{34, 35}

Experimental Section

Materials. Bioglass precursor sols were obtained by mixing 56 mL of commercial milk (Ca(II) 30 mM, P(V) 30 mM, K(I) 44 mM, Na(I) 21 mM), 12.5-35 mL of Ludox[®] HS-40 (aqueous suspension of 12 nm SiO₂ nanoparticles, 40% weight volume) and an extra amount of water to obtain a final volume of 100 mL. Samples were labeled ML05 to ML14 according to the final weight percentage of silica (5-14%) in the parent sol. *ISISA protocol:* suspensions were loaded into the insulin syringes molds (length 80 mm, diameter 4 mm), then were unidirectionally frozen by dipping the molds at defined rates into a -196 °C (liquid nitrogen) cold bath. The unidirectional frozen samples were freeze-dried using an Alpha 1-2 LD Plus freeze-drier. The green monoliths were finally annealed at 873-1273 K (air atmosphere, 10 K min⁻¹) and held at the final temperature for 5 h.³⁸ Pore dimension and wall thickness of monoliths were determined from FESEM micrographs of cross sections to the direction of freezing. For each construct, at least 20 measurements of the pore width and wall thickness were made on each micrograph, to provide a representative mean value and standard deviation.

***In vitro* bioactivity test.** The assessment of the *in vitro* bioactivity of the annealed scaffolds was carried out in a simulated body fluid (SBF) solution composed by NaCl, KCl, K₂HPO₄·3H₂O, MgCl₂·6H₂O, CaCl₂, and Na₂SO₄ into distilled water and buffering at pH 7.3 with tris (hydroxymethyl) aminomethane H₂N-C(CH₂OH)₃ and HCl, according to well established formulations.³⁹ Each specimen (0.1 g) was immersed in 100 mL of SBF contained in polyethylene vials at 37°C under sterile conditions for increasing periods of time (0-7 days). Once removed from the incubation solution, the samples were rinsed gently firstly in ethanol and then using deionized water, and left to dry at ambient temperature in a desiccator for further characterization. The sample's evolution was analyzed by scanning electron microscopy (SEM Zeiss Supra-40) coupled with EDS probe, Fourier transform infrared (FTIR, NICOLET 8700 20 SXC) and PXRD (Siemens D5000, Ni-filtered Cu K_α radiation). The thermal analysis was performed using a TG50 Shimadzu balance with a heating rate of 10 K min⁻¹ under air atmosphere (50 mL min⁻¹).

Results and discussion

It is known that the versatility offered by ISISA process lies in the possibility of tuning the monolith's macroporous texture with several physiochemical parameters.⁴⁰ Among them, the most relevant are: solvent/s composition, solute/s nature (size, morphology, charge) and concentration, freezing rate and temperature gradient.¹² In the present study, the preparation of bioglass monolithic scaffolds was restricted to the use of water as the only solvent and the thermal gradient was established between ambient (298 K) and liquid N₂ (77 K); samples were typically immersed at 2 mm min⁻¹. Concerning to the overall sample composition, several Ludox[®] to milk ratios were chosen to study the textural modification, exclusively. Sample ML10 in particular was extensively studied in terms of texture, thermal stability and biomineralization behavior. That particular formulation resulted in a 98:1:1 Si(IV):P(V):Ca(II) overall molar composition; certain alternative milk to silica ratios were also explored, as well as freezing rates. The resulting monoliths kept both the shape and the size of the employed container, in

which the starting Ludox[®]-milk sol was confined prior to ISISA. Since the ice-front progress reached a constant speed (e.g., nominal) at the upper half of the monolith, all the experiments were conducted on that portion, exclusively.⁴¹ Typically, sol-gel based bioglass precursors are dried and then submitted to an oxidative annealing step at 773 K, after which both the remnant salts, acids, eventual organic residues and/or molecular templates are decomposed. In the present case, TGA analysis revealed the massive departure of organic components after annealing at 723 K, irrespective of the Ludox[®] to milk ratio (see figure S1). Figure 1 depicts FESEM images of samples after annealing in air at 873 K presented a homogeneous macroporosity in the range of tens of micrometers, commonly observed in these systems.⁴²

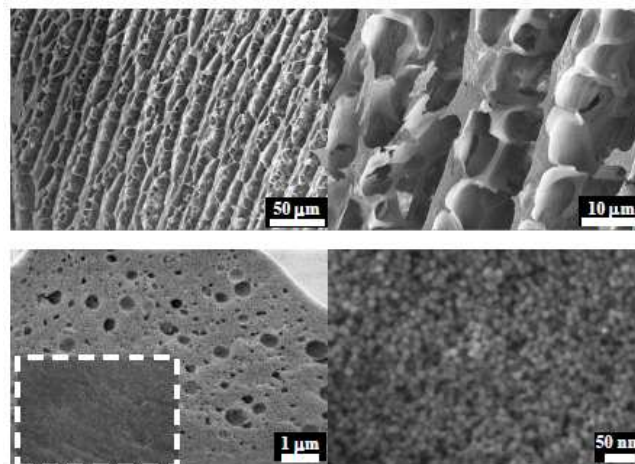
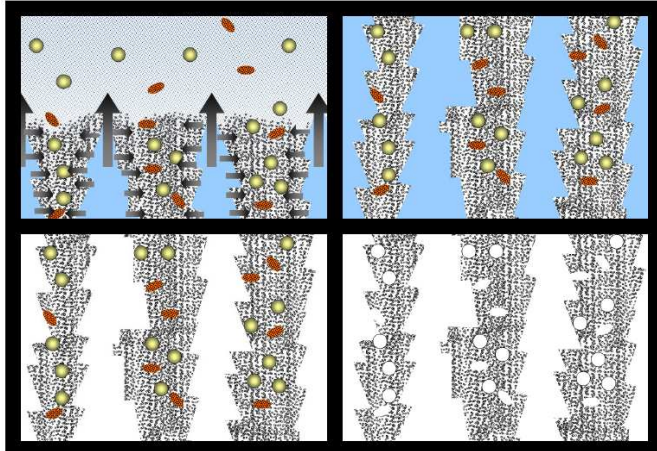


Fig. 1. FESEM images of cross-sectioned ML10 sample (perpendicular to the freezing direction) monolithic scaffold prepared with a freezing rate of 2 mm min⁻¹, annealed for 5 h at 873 K. Inset (bottom left) depicts the texture resulting from the milk-free Ludox[®] control prepared under identical procedure.

The texture is built by parallel array of lamellae, periodically segmented by perpendicular secondary bridges. Their transversal section revealed a regular pore pattern; a small region a few microns close to the external surface of the mold is affected by the inherent freezing features of this method (not shown).¹¹ Both macroporosity and wall's thickness remained unaltered after thermal treatment, while submicrometric pores belonging to the former templating entities (milk lipid vesicles and soluble proteins) appeared within the walls after thermal treatment (see Figure S3). These templates were effectively dispersed in-between silica nanoparticles along ISISA; after mineralization of milk's moieties, a new level of porosity in the 50-200 nm range was achieved. In the absence of milk, more dense walls were obtained, only exhibiting the lowest level of porosity originated by the empty voids left in between Ludox[®] nanoparticles. There was no evidence of segregation of micrometric Ca(II) phosphate crystalline phases, suggesting the high degree of dispersion of both Ca(II) and P(V) within the SiO₂ scaffold. Then, in a single macroscopic piece, three levels of porosity coexist due to the simultaneous templating effect of ice (macropores), milk (50-200 nm mesopores) and the voids left between preformed Ludox[®] nano building blocks (2-5 nm mesopores).

In contrast with related sol-gel based silica systems,⁴³ the lack of well-defined hexagonal pores, even for the lowest freezing rates explored could be ascribed to the precursors composition; milk's soluble moieties (salts and macromolecules) can affect

the growth and the resulting morphology of ice crystals. However, the obtained texture is well preserved all along the sample's volume, without the occurrence of radial heterogeneity or massive cracks.¹¹ Scheme 1 summarizes the key steps involved in the scaffold's structuration.



Scheme 1. Upper left panel: aqueous suspension containing Ludox[®] (black dots), milk's solutes as liposomes (yellow spheres) and proteins (orange globules); vertical freezing front of dendritic ice (blue area) and lateral segregation milk's solutes and Ludox[®] away from ice walls (light blue area). Upper right panel: massive segregation of ice and solutes phases. Lower left panel: sublimation of ice leaving empty voids (white area). Lower right panel: hierarchical scaffold obtained after thermal decompositions of liposomes and proteins; partial sintering of Ludox[®].

Concerning the effect of annealing over templated bioglasses, an extra step beyond milk's mineralization can be expected. This step involve the solid state consolidation of the bioglass itself takes place through the diffusion of Ca(II), K(I) and P(V) ions towards SiO₂ domains, as well as the sintering of Ludox[®] nanoparticles. However, if the hierarchical features obtained are aim to be preserved, massive sintering and the subsequent pore's collapse must be avoided. Then, the annealing temperature was explored in the 873-1273 K range, in order to assess the range of texture's stability.^{38, 44} Differential thermal analysis revealed that either samples constituted by bare Ludox[®] nanoparticles or Ludox[®]-milk mixtures (previously mineralized at 773 K under air atmosphere) consumed heat during sintering process, with a maximum centered at 1150 K, in agreement with the glass transition temperature observed for related systems (see figure S2).¹⁴ Then, a FESEM screening was performed over samples annealed within the 873-1273 K range, taking representative images of the resulting textures.

In contrast with sol-gel based silica, the dense silica nanoparticles employed herein remain stable towards sintering after annealing at 973 K (see figure 2, S3). Once annealed at 1073 K, massive sintering process takes place and both interparticle and milk-templated intrawall mesopores collapse and disappear. The subsequent densification of formerly mesoporous walls results in a net scaffold's contraction. However, the lack of material within the walls results in a micrometric porosity (globular windows) that replace the former mesopores; giving rise to a bimodal hierarchy. After further annealing up to 1273 K these windows collapse in great extent and only a strictly macroporous scaffold

remains. The net process involves a densification of the scaffold as a whole.

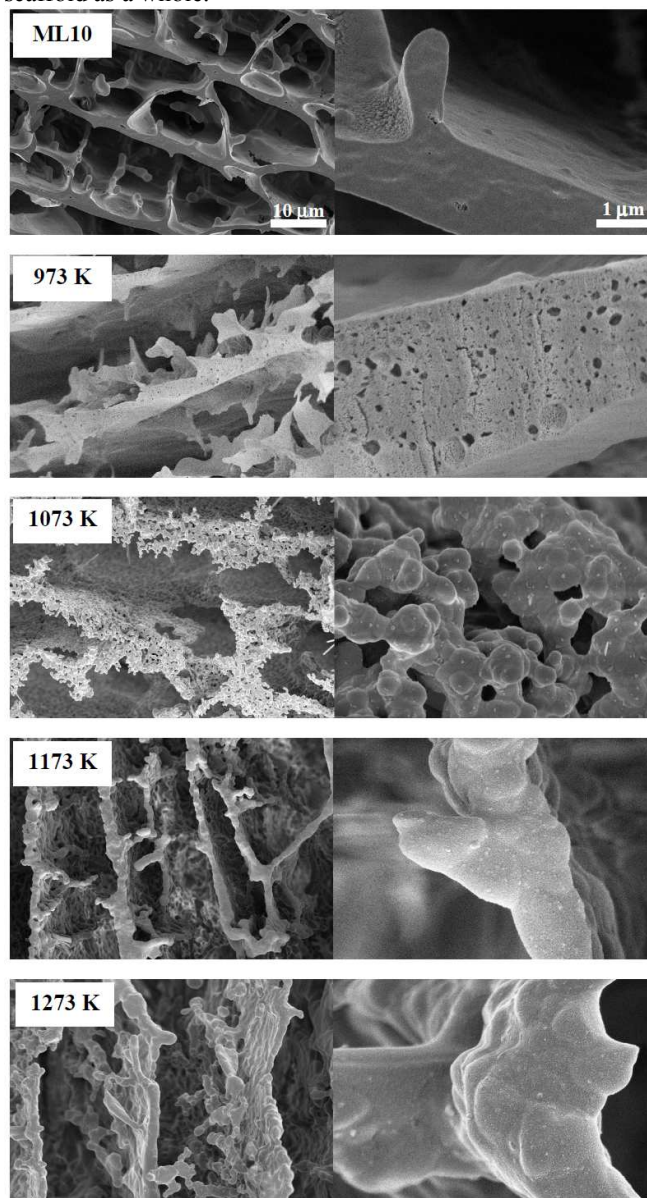


Fig. 2. FESEM images of sample ML10 prepared with a freezing rate of 2 mm min⁻¹ annealed for 5 h at increasing temperatures under air atmosphere.

Nitrogen sorption isotherms revealed that after annealing at 773 K, most of the scaffold's surface and intra-wall porosity (biotemplated voids and inter particle voids) is accessible. A maximum value was reached after annealing at 873 K, probably due to the departure of remnant organic residues. The surface area value is slightly smaller than the maximum geometrical area expected for non-sintered Ludox[®] nanoparticles of 12 nm diameter, confirming the lack of significant sintering among them. However, once annealed at 973 K this latter effect is noticeable, since the surface area decay, while middle-range pores (150-250 nm) remain almost invariant (see figure 3, S5-7). After annealing at 1073 K, massive collapse of porosity and surface confirms the effective sintering of scaffold's walls, in agreement with FESEM inspection.

Concerning the effect of annealing from a chemical point of view, representative annealed ML10 samples and their correspondent controls were analyzed by means of PXRD. Within the explored temperature range, both ML10 samples as well as bare Ludox[®] control remain amorphous, exhibiting the characteristic broad peak centered at 22 degrees, exclusively (see figure 4). No signals belonging to crystalline phases coming from milk oxides/phosphates were observed, suggesting a high degree of interspersions of these minerals within the silica scaffold. Notwithstanding, no crystalline Ca(II) or Ca(II)-Na(I) silicates, inherent to related bioglass compounds were observed either.³⁸

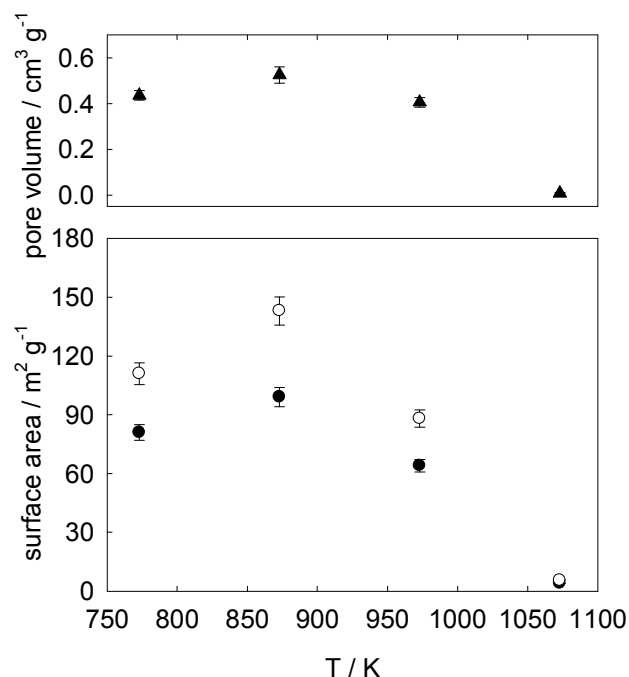


Fig. 3. Pore volume (upper panel) and surface area (lower panel) determined by Langmuir, (empty circles) or BET (filled circles) methods observed for sample ML10 annealed for 5 h at increasing temperatures.

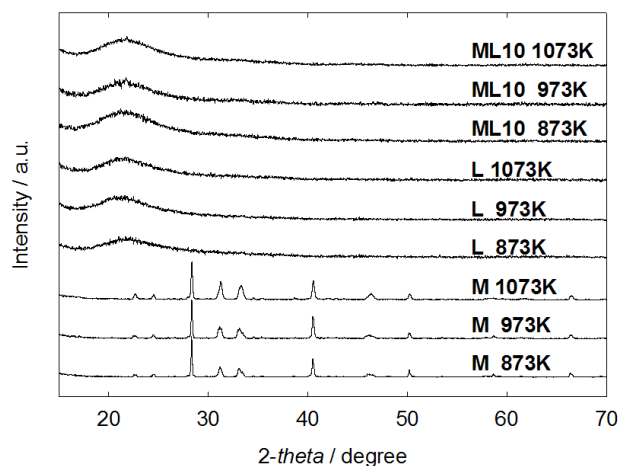


Fig. 4. PXRD patterns of bare milk (M), Ludox[®] (L) and milk-Ludox[®] ML10 samples annealed for 5 h at 873-1073 K under air atmosphere.

The evolution of the most significant textural parameters of each sample was described by means of the pore's major and minor dimension and the wall thickness. Figure 5 compiles the evolution of the aforementioned parameters observed for the annealed samples, prepared with increasing contents of Ludox[®]. In general terms, the green scaffold's texture follows the expected trend, in which the solid's content exerted a marked influence on both pore's size and shape. The wall thickness remains one order of magnitude smaller than the pore size, achieving a cellular like aspect. Low rates allow the formation of bigger ice crystals, giving birth to oblong pores with the longer dimension almost doubling the shorter one; then both dimensions were taken into account.

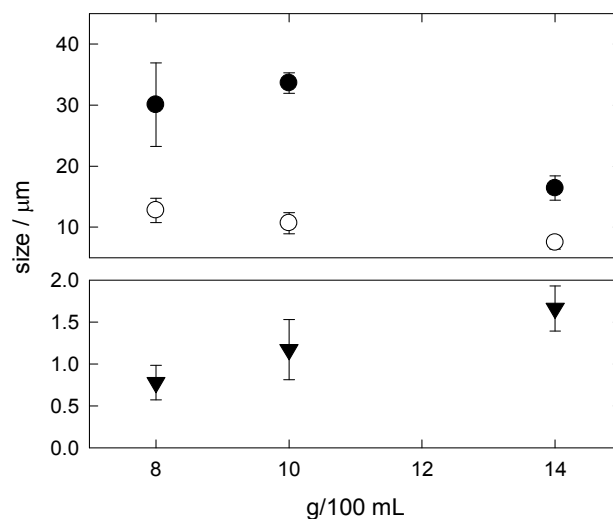


Fig. 5. Minor pore section (empty circles), major pore section (filled circles) and wall average thickness (triangles) of ML scaffolds prepared with a freezing rate of 2 mm min⁻¹ with increasing Ludox[®] content (g/100 mL) in the starting sol.

Once the monoliths are annealed, their macroscopic dimensions are almost preserved; the micrometric texture, depending on the preparation conditions, can be significantly tuned.

The effect of freezing rate in the resulting structure was explored; samples ML10 and ML14 were prepared employing two-fold freezing speed of 4 mm min⁻¹. Sample ML10 remained almost invariant respect from the original preparation, while sample ML14 exhibited macropores reduced to almost a half of their original size (see figure S4). Then, scaffolds structure can be effectively tuned with this variable for certain compositions. In general, for a certain freezing conditions, both solute's diffusion coefficient and its inherent solubility affects the spatial frequency in which the ice crystal, say the pores, occurs.³⁴ Since the freezing rate can be easily tuned and modified for a given sample, this process is promising in the preparation on monolithic pieces with a porosity gradient,⁴⁵ that in principle should tune and control the cellular response to these scaffolds.^{46, 47} Being established the influence on the structure of the typical preparative parameters, we focused our attention on a key chemical aspects related with the proposed method.

Mineralization behavior

In order to evaluate the potential bioactivity of the obtained bioglass scaffolds, representative annealed at 873 K samples

were submitted to a well-established in vitro bioactivity assay, based on the incubation of bioglasses in SBF at 37 °C for increasing immersion periods. After 4 h long exposure, FESEM inspection revealed the presence of scarce spheroidal particles of 50-150 nm, well dispersed along the scaffold's surface. The extension of exposure to 1 d allowed the development of a much denser coating, well distributed along the surface. The deposit was mainly constituted by rosettes of 200-400 nm, typically observed after $\text{Ca}_5(\text{PO}_4)_3\text{OH}$ (hydroxyapatite, HA in the following) crystallization onto bioglasses.³¹ In contrast with sol-gel based counterparts, the present bioglasses develop less homogeneous coatings, presumably due to the inherent differences of this method. The former distributes both P(V) and Ca(II) in much higher amount and at a molecular level; the latter concentrates both elements in the zones where phospholipids and amorphous Ca(II)-phosphate/caseinate were confined during ISISA, respectively. However, the present method achieves a good level of biomineralization in very short periods (see table S1); after 7 d exposure the deposits remained similar, both in texture and composition, to those obtained after 24 h, suggesting that most of the biominerals load of the parent scaffold reacts along the first day of exposure. The partially sintered Ludox[®] building units as well as the templated mesopores remained stable with no signs of erosion, confirming the effective partial sintering of nanoparticles after thermal consolidation.

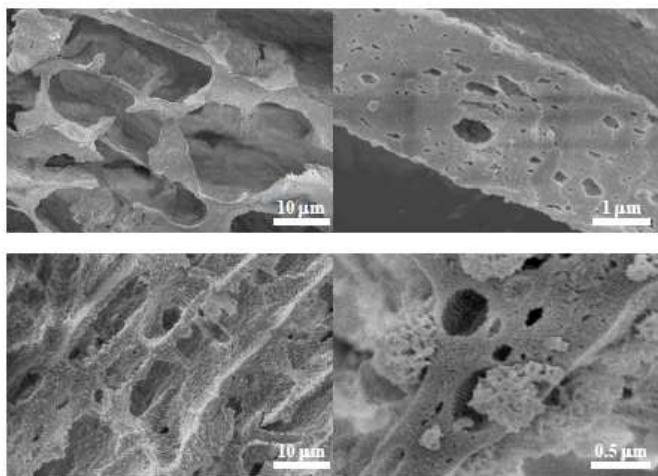


Fig. 6. FESEM images of cross-sectioned (perpendicular to the direction of freezing) monolithic ML10 scaffold prepared with a freezing rate of 2 mm min⁻¹, exposed to SBF for 4 h (upper row) and 24 h (lower row).

The chemical nature of the deposited layer was estimated by means of SEM-EDS probe (see figure S8). After a 4h-long exposure, both Ca and P were present at a level of traces, as in the pristine scaffold, in excellent agreement with the original milk formulation. However, after 24 h exposure the content of both elements increased markedly while the Ca/P ratio was ca 1.3±0.3, close to that of HA, as was anticipated by FESEM inspection. Sample ML10 annealed at 1273 K revealed no signs of biomineralization after similar treatment, indicating the massive redistribution of biominerals. The evolution of samples exposed to SBF was inspected by means of FTIR spectroscopy analyses. The FTIR spectra revealed main bands composed by the signals centered at 950, 1100, and 1200 cm⁻¹, related to the Si-O-Si and P-O stretching of silica glass and a shoulder at about 900 cm⁻¹ related to the Si-O-Ca vibrational modes (data not shown). The peak centered at 450 cm⁻¹ accounts for the Si-

O-Si bending of silica glass.⁴⁸ After mineralization with SBF, a couple of well-defined additional peaks centered at 598 and 566 cm⁻¹ became noticeable, corresponding to P-O bending vibrations of apatite-like phases (see HA reference).^{49, 50} Sample ML05 developed biomineralization signals at a faster rate than ML10 one; this is expectable since the milk to silica ratio of the former doubles the latter.

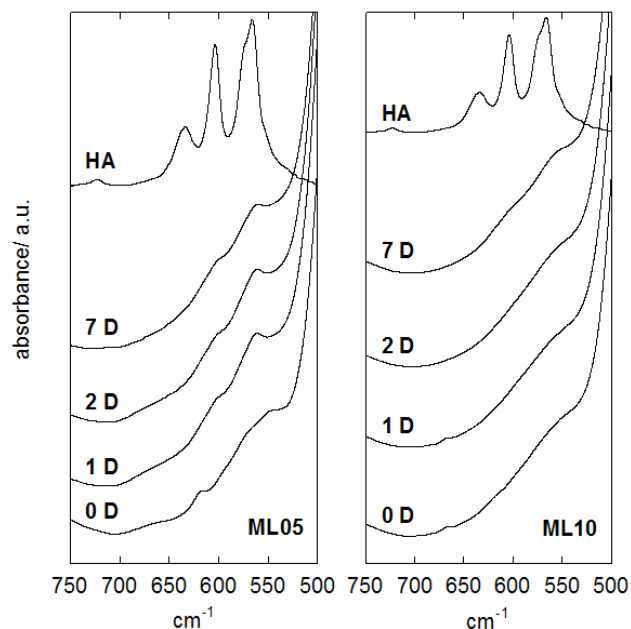


Fig. 7. FTIR spectra of ML05 (left) and ML10 (right) scaffolds exposed to simulated body fluid (310 K) for 0-7 days. Hydroxyapatite (HA), $\text{Ca}_5(\text{PO}_4)_3\text{OH}$, reference is also included.

For highly homogeneous bioglasses, it is accepted that exposure to SBF drives surface dissolution process. Then, both Ca(II) and P(V) concentration in solution continuously increases, rising the supersaturation respect to HA up to a critical value, in which nucleation and growth of that phase takes place onto the exposed surface.¹⁵ After that initial step, that usually takes a week for dense bioglasses,^{14, 51, 52} the solution composition remains almost invariant, even when the HA layer is still developing.¹⁵ However, being a mass transport affected process, the bioglass texture could influence biomineralization kinetics as was reported for high surface mesoporous bioglasses^{53, 54} or nanofiber shaped ones,²⁸ in which the initial step can be reduced to several hours. Previous studies performed over analogous structures prepared by sol gel revealed that the transport properties are not controlling the biomineralization process. However, those samples were formulated with much higher overall Ca(II) and P(V) loadings than in the present case.⁵⁵ Therefore, the extremely fast biomineralization response observed herein can be attributed to the inherently well distributed biominerals present in the parent scaffold's surface.

Conclusions

The ISISA based texture tune of Ludox[®]-milk suspensions opened the gate for the preparation of hierarchical bioglass scaffolds. The inherently complex texture was essentially preserved after a mild annealing while the chemical homogeneity was enough to ensure a fast in vitro biomineralization response, without disrupting the achieved hierarchical structure. This alternative approach, inspired in the

well-established sol-gel chemistry of bioglasses, illustrated a bioinspired route for the obtainment of more accessible and greener biomaterials.

Acknowledgements

This work was supported by the University of Buenos Aires (UBACyT 20020130100610BA), by Agencia Nacional de Promoción Científica y Tecnológica (ANPCyT PICT 2012-1167), and by National Research Council of Argentina (CONICET PIP 11220110101020). YM acknowledge CONICET for postdoctoral fellowship. MJ is a Research Scientist of CONICET (Argentina).

Notes and references

^a Laboratorio de Superficies y Materiales Funcionales INQUIMAE-DQIAQF, Facultad de Ciencias Exactas y Naturales, Universidad de Buenos Aires, Ciudad Universitaria Pab. II, C1428EHA, Buenos Aires (Argentina). E-mail: jobbag@qi.fcen.uba.ar

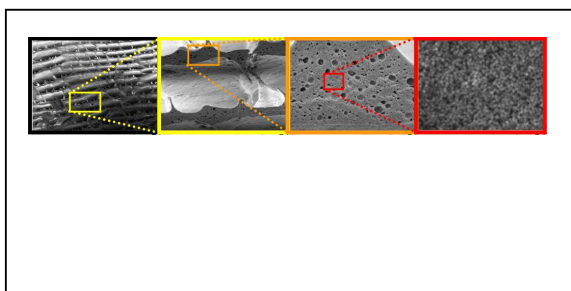
Electronic Supplementary Information (ESI) available: See DOI: 10.1039/b000000x/

References

- L. L. Hench, *J. Mater. Sci.-Mater. Med.*, 2006, **17**, 967-978.
- D. Arcos and M. Vallet-Regi, *Acta Biomater.*, 2010, **6**, 2874-2888.
- J. R. Jones, *Acta Biomaterialia*, 2013, **9**, 4457-4486.
- R. M. Day, A. R. Boccaccini, S. Shurey, J. A. Roether, A. Forbes, L. L. Hench and S. M. Gabe, *Biomaterials*, 2004, **25**, 5857-5866.
- R. M. Day, *Tissue Eng.*, 2005, **11**, 768-777.
- I. D. Xynos, A. J. Edgar, L. D. K. Buttery, L. L. Hench and J. M. Polak, *J. Biomed. Mater. Res.*, 2001, **55**, 151-157.
- I. D. Xynos, M. V. J. Hukkanen, J. J. Batten, L. D. Buttery, L. L. Hench and J. M. Polak, *Calcif. Tissue Int.*, 2000, **67**, 321-329.
- J. A. Roether, A. R. Boccaccini, L. L. Hench, V. Maquet, S. Gautier and R. Jerome, *Biomaterials*, 2002, **23**, 3871-3878.
- M. C. Gutierrez, M. Jobbagy, N. Rapun, M. L. Ferrer and F. del Monte, *Adv. Mater.*, 2006, **18**, 1137-1140.
- M. C. Gutierrez, Z. Y. Garcia-Carvajal, M. Jobbagy, L. Yuste, F. Rojo, C. Abrusci, F. Catalina, F. del Monte and M. L. Ferrer, *Chem. Mater.*, 2007, **19**, 1968-1973.
- M. C. Gutierrez, Z. Y. Garcia-Carvajal, M. Jobbagy, T. Rubio, L. Yuste, F. Rojo, M. L. Ferrer and F. del Monte, *Adv. Funct. Mater.*, 2007, **17**, 3505-3513.
- M. C. Gutierrez, M. L. Ferrer and F. del Monte, *Chem. Mater.*, 2008, **20**, 634-648.
- M. C. Gutiérrez, M. Jobbagy, M. L. Ferrer and F. Del Monte, *Chem. Mater.*, 2008, **20**, 11-13.
- J. R. Jones, L. M. Ehrenfried and L. L. Hench, *Biomaterials*, 2006, **27**, 964-973.
- C. Ohtsuki, T. Kokubo and T. Yamamuro, *J. Non-Cryst. Solids*, 1992, **143**, 84-92.
- K. Rezwani, Q. Z. Chen, J. J. Blaker and A. R. Boccaccini, *Biomaterials*, 2006, **27**, 3413-3431.
- T. Kokubo, H. M. Kim and M. Kawashita, *Biomaterials*, 2003, **24**, 2161-2175.
- X. X. Yan, C. Z. Yu, X. F. Zhou, J. W. Tang and D. Y. Zhao, *Angew. Chem. Int. Edit.*, 2004, **43**, 5980-5984.
- A. Lopez-Noriega, D. Arcos, I. Izquierdo-Barba, Y. Sakamoto, O. Terasaki and M. Vallet-Regi, *Chem. Mat.*, 2006, **18**, 3137-3144.
- D. Arcos, A. Lopez-Noriega, E. Ruiz-Hernandez, O. Terasaki and M. Vallet-Regi, *Chem. Mater.*, 2009, **21**, 1000-1009.
- T. A. Ostomel, Q. H. Shi, C. K. Tsung, H. J. Liang and G. D. Stucky, *Small*, 2006, **2**, 1261-1265.
- S. R. Hall, D. Walsh, D. Green, R. Oreffo and S. Mann, *J. Mater. Chem.*, 2003, **13**, 186-190.
- J. R. Jones, O. Tsigkou, E. E. Coates, M. M. Stevens, J. M. Polak and L. L. Hench, *Biomaterials*, 2007, **28**, 1653-1663.
- X. Han, X. F. Li, H. M. Lin, J. Ma, X. Chen, C. H. Bian, X. D. Wu and F. Y. Qu, *J. Sol-Gel Sci. Technol.*, 2014, **70**, 33-39.
- J. M. Qian, Y. H. Kang, Z. L. Wei and W. Zhang, *Mater. Sci. Eng. C-Biomimetic Supramol. Syst.*, 2009, **29**, 1361-1364.
- N. Li, Q. Jie, S. M. Zhu and R. D. Wang, *Mater. Lett.*, 2004, **58**, 2747-2750.
- N. Li, Q. Jie, S. M. Zhu and R. D. Wang, *Ceram. Int.*, 2005, **31**, 641-646.
- H. W. Kim, H. E. Kim and J. C. Knowles, *Adv. Funct. Mater.*, 2006, **16**, 1529-1535.
- H. S. Yun, S. E. Kim and Y. T. Hyeon, *Chem. Commun.*, 2007, 2139-2141.
- H. S. Yun, S. E. Kim, Y. T. Hyun, S. J. Heo and J. W. Shin, *Chem. Mater.*, 2007, **19**, 6363-6366.
- Y. Minaberry and M. Jobbagy, *Chem. Mater.*, 2011, **23**, 2327-2332.
- J. W. Kim, K. Tazumi, R. Okaji and M. Ohshima, *Chem. Mater.*, 2009, **21**, 3476-3478.
- S. R. Mukai, H. Nishihara and H. Tamon, *Microporous and Mesoporous Materials*, 2008, **116**, 166-170.
- H. Nishihara, S. Iwamura and T. Kyotani, *J. Mater. Chem.*, 2008, **18**, 3662-3670.
- S. Deville, *Adv. Eng. Mater.*, 2008, **10**, 155-169.
- S. Deville, E. Maire, G. Bernard-Granger, A. Lasalle, A. Bogner, C. Gauthier, J. Leloup and C. Guizard, *Nat. Mater.*, 2009, **8**, 966-972.
- S. Deville, E. Maire, A. Lasalle, A. Bogner, C. Gauthier, J. Leloup and C. Guizard, *J. Am. Ceram. Soc.*, 2009, **92**, 2489-2496.
- A. R. Boccaccini, Q. Chen, L. Lefebvre, L. Gremillard and J. Chevalier, *Faraday Discuss.*, 2007, **136**, 27-44.
- T. Kokubo and H. Takadama, *Biomaterials*, 2006, **27**, 2907-2915.
- S. Deville, *J. Mater. Res.*, 2013, **28**, 2202-2219.
- S. Deville, E. Saiz and A. P. Tomsia, *Acta Mater.*, 2007, **55**, 1965-1974.
- M. J. Hortiguera, M. C. Gutierrez, I. Aranaz, M. Jobbagy, A. Abarrategi, C. Moreno-Vicente, A. Civantos, V. Ramos, J. L. Lopez-Lacomba, M. L. Ferrer and F. del Monte, *J. Mater. Chem.*, 2008, **18**, 5933-5940.
- H. Nishihara, S. R. Mukai, D. Yamashita and H. Tamon, *Chem. Mater.*, 2005, **17**, 683-689.
- D. Arcos, D. C. Greenspan and M. Vallet-Regi, *Chem. Mater.*, 2002, **14**, 1515-1522.
- O. Bretcanu, C. Samaille and A. R. Boccaccini, *J. Mater. Sci.*, 2008, **43**, 4127-4134.
- M. C. von Doernberg, B. von Rechenberg, M. Bohner, S. Grunfelder, G. H. van Lenthe, R. Muller, B. Gasser, R.

Journal Name

- Mathys, G. Baroud and J. Auer, *Biomaterials*, 2006, **27**, 5186-5198.
47. S. J. Hollister, *Nat. Mater.*, 2005, **4**, 518-524.
48. M. M. Pereira, A. E. Clark and L. L. Hench, *J. Biomed. Mater. Res.*, 1994, **28**, 693-698.
49. B. O. Fowler, *Inorganic Chemistry*, 1974, **13**, 207-214.
50. B. O. Fowler, *Inorganic Chemistry*, 1974, **13**, 194-207.
51. J. Andersson, E. Johannessen, S. Areva, N. Baccile, T. Azaïs and M. Lindén, *J. Mater. Chem.*, 2007, **17**, 463-468.
52. J. Lao, J. M. Nedelec and E. Jallot, *J. Phys. Chem. C*, 2008, **112**, 9418-9427.
53. A. López-Noriega, D. Arcos, I. Izquierdo-Barba, Y. Sakamoto, O. Terasaki and M. Vallet-Regí, *Chem. Mater.*, 2006, **18**, 3137-3144.
54. X. Yan, X. Huang, C. Yu, H. Deng, Y. Wang, Z. Zhang, S. Qiao, G. Lu and D. Zhao, *Biomaterials*, 2006, **27**, 3396-3403.
55. C. Ohtsuki, T. Kokubo, K. Takatsuka and T. Yamamuro, *J. Ceram. Soc. Jpn.*, 1991, **99**, 1-6.



Low cost hierarchical bioglass scaffolds were prepared by freeze drying cow milk loaded with SiO₂ nanoparticles.